VIRTUAL REALITY MEDICAL TRAINING WITH FORCE FEEDBACK

Honors Undergraduate Thesis Submitted to:

The College of Engineering Honors Committee
College of Engineering
122 Hitchcock Hall
The Ohio State University

by:

David A. Moody
Department of Mechanical Engineering
Spring 2005
******

Approved by:

_____

Dr. Marcelo J. Dapino, Advisor
Department of Mechanical Engineering

ACKNOWLEDGEMENTS

This research project was conducted at the Smart Materials and Structures Lab (SMSL) at The Ohio State University from summer 2004 to spring 2005. I am extremely grateful to the College of Engineering for providing financial support for this undergraduate honors research project.

I would like to begin by thanking my advisor, Professor Marcelo J. Dapino of the Mechanical Engineering Department for his overwhelming support and guidance throughout the duration of this project. I would also like to thank Dr. Don Stredney and all the team members at the Ohio Supercomputer Center (OSC) for all the help and support throughout the duration of this project. In addition, I would like to extend a special thanks to all my SMSL buddies for their assistance with testing and other aspects of this project. I also would like to thank Keith Rogers and Gary Gardner from the Mechanical Engineering machine shop and I would like to thank Vijay Neelakantan who was instrumental in helping me with the control for the device.

In closing, I would like to express my deepest gratitude to my mother and father Curtis and Elaine Moody for all the love and support they have given me not only during this project but throughout my entire life, I hope I make you proud. I would also like to thank my friends Deonte' Tyson, Nadia Anguiano, Raymond Armstead Jr., and Bill Ross for encouragement they have given me throughout my undergraduate career. Finally, I would like to thank my brothers Curtis and Jonathan for picking up my chores around the house while I was writing this thesis, thank you.

VITA

March 17, 1982……..…Born

2000…..…….Graduated from Northland High School, Columbus, Ohio

2000-Present……..……..Undergraduate Student
Department of Mechanical Engineering
The Ohio State University

June 12, 2005……..B.S. Mechanical Engineering
The Ohio State University

Table of Contents

List of Figures

List of Symbols

Symbol	Description	Unit
A_{gap}	Cross sectional area of gap of magnet	[m^2]
F_{mag}	Force from electromagnet	[N]
F_u	User input force	[N]
i	Current	[A]
L	Inductance of coil	[H]
M	Number of turns of coil	[-]
m	Mass of steel shaft	[kg]
μ_1	Friction constant from bearings	[-]
μ_2	Friction constant from brass-shaft interaction	[-]
μ_o	Magnetic permeability of air	[-]
N	Normal force	[N]
R	Resistance	[Ohm]
V	Voltage	[V]
x	Displacement of magnet	[m]
z	Displacement of shaft	[m]
ż	Velocity of shaft	[m/s]

Chapter 1

INTRODUCTION

1.1 Motivation

There is a critical need for novel tools to allow training of industry personnel quickly, safely, and effectively such that the trainees can retain skills and become proficient at their craft less expensively. Virtual reality (VR) has been shown to enable novel training solutions in many fields, including the automotive industry, military, construction, and agriculture. Training simulators have been developed that use VR software in combination with force feedback devices composed of electric motors and cables. These systems allow users to interact with a computer-simulated environment and have force-feedback (haptic) devices which mimic the tactile sensations associated with the physical system being simulated.

This study is concerned with the development of a haptic device for simulation of epidural needle insertion procedures. Because of the broad range of forces involved in these types of procedures, the use of a cable-operated manipulators leads to reduced fidelity and associated bandwidth due to cable compliance. The bandwidth of a device is the range in which it can accept or reject signals. In the medical applications being considered, the signal is the medical trainee using a surgical tool on a patient. The responsibility of the haptic device is to respond to the medical trainee's surgical tool with various distinct forces associated with various types of tissues involved in the procedure. The study is therefore focused on the development of an alternative technology which overcomes the fidelity limitations of cable-operated devices to simulate and epidural needle insertion in VR.

During an epidural treatment, a local anesthetic is administered in a sufficient dosage into the epidural space to result in an interruption of the passage of sensory, motor, and autonomic impulses in both the dorsal and ventral spinal roots [1-3]. This leads to a reduction in pain during the birthing process for expecting mothers. Two different approaches are used to perform this procedure, the median (skin and tissue) approach and the paramedian (skin, tissue, and bone) approach. The former is used more commonly [4]. Side effects from improper procedure include trauma, minor to major headaches, infection, and toxic ischemia [1-2], [4-5]. Performing a successful epidural treatment requires not only a thorough knowledge of the anatomy of the effect of needle placement, but significant experience. The latter requirement emphasizes the importance of reliable, accurate and consistent training tools. The following quote highlights the importance of experience.

> "In the hands of skilled clinicians, serious complications are infrequent and moreover, idiosyncratic in that their incidence does not appear to correlate strongly with a single technique." [5]

Training medical residents in the virtual environment presents several advantages. At The Ohio State University, training of each medical resident currently costs $70,000 over the duration of the medical program. If part of the training could be performed in the virtual environment, significant reduction in cost could be achieved. Another consideration is insufficient number of volunteers to accommodate the number of training procedures associated with a large population of medical residents. This surely is compounded by the intrinsic risks involved in the epidural procedure.

1.2 Objective

The objective of this project is to develop an improved haptic device for realistic medical training of epidural needle insertion. The design must be able to simulate both the median and paramedian approaches of an epidural. Current haptic devices are unable to simulate bone contact which is critical for the paramedian approach. It is believed that a force of 20 N will simulate bone contact, therefore the force bandwidth of the system must range from 0 – 20 Newtons. This project uses an electromagnet to achieve the goal of developing a haptic device that will provide a larger bandwidth, high fidelity, and appropriate force feedback in VR simulations.

Chapter 2

General Aspects of Electromagnets

2.1 Electromagnets

One of the many unique discoveries in physics was when Faraday discovered that a magnetic field can be produced in a ferromagnetic material by wrapping the material with wire and applying an alternating or constant electrical current to the coil [7]. The magnetic field induced by an electrical current can be seen in Fig 2.1. When a magnetic yoke is fixed within the coil and a movable magnetic piece (moving iron) is placed in a proximity to the yoke, the system is called an electromagnet.

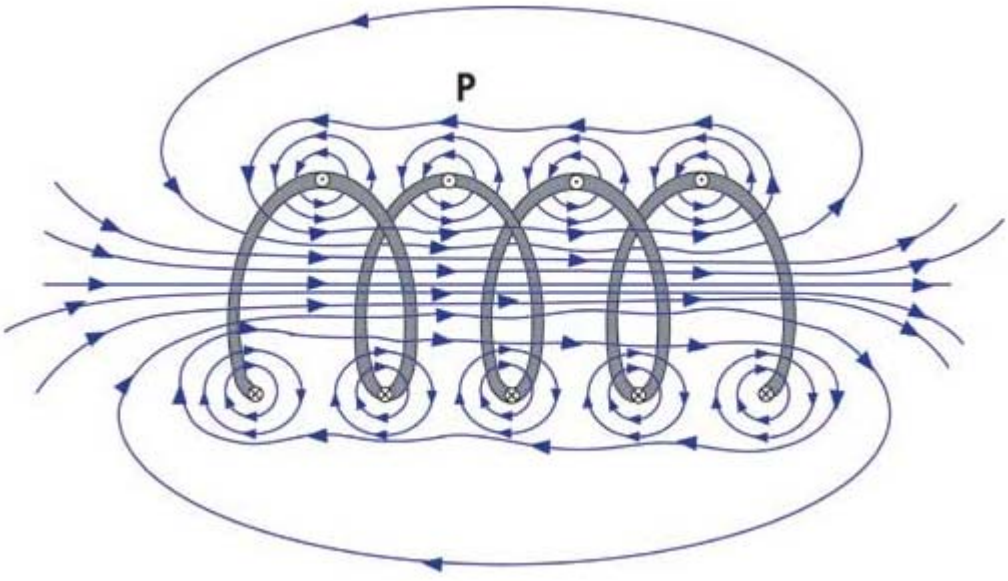

Figure 2.1: Lines of magnetic flux in an air electromagnet.

When a current is applied to the electromagnet, a magnetic force is produced on the moving iron which is a function of the magnetic flux and magnetic circuit reluctance R(x), where x is the distance between the yoke and moving iron. The reluctance (2.1.1) is a measure of the resistance to magnetic flux, much like resisters provide resistance to currents flow, the reluctance relation is given by

$$R(x) = \frac{x}{\mu_o A_{gap}} \tag{2.1.1}.$$

Where μ_o is the permeability of free space and A_{gap} is the cross sectional area of the flux path. The intensity of the magnetic flux is

$$\phi = \frac{Mi}{R(x)} \tag{2.1.2}.$$

With M turns in the coil and i the current flowing through it. As the reluctance increases the flux increases. Combing equations (2.1.1) and (2.1.2), the magnitude of the force produced by the magnetic piece is give by

$$\left|F_{mag}\right| = \frac{\phi^2}{2}\frac{dR(x)}{dx} = \frac{(MV)^2 \mu_o A_{gap}}{2(xR)^2} \tag{2.1.3}.$$

It is noted that the direction of the force acting on the moving iron is towards the electromagnet [8].

Chapter 3

Brake Mechanism Design

3.1 Brake System

Having chosen an electromagnet to be the actuator for the system, the next step was to design a friction braking system that would ensure authentic simulation of an epidural in a virtual environment. The brake mechanism designed to simulate the epidural is shown in Fig 3.1. A brass block applies friction to the shaft that induces the force felt by the user during the simulation. A brass block was chosen to apply the friction to the shaft for two reasons. First, brass is softer than steel and thus it can not scratch the surface of the steel shaft; and second, brass has adequate friction qualities. Despite other materials such as aluminum, which has a higher coefficient of friction on steel than brass, in our tests, brass

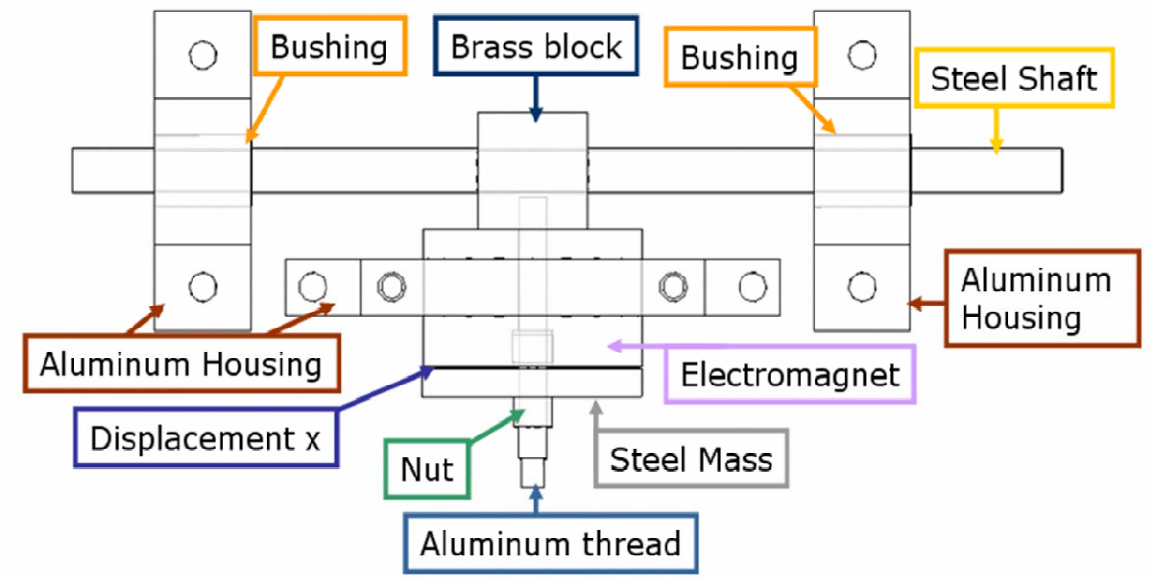

Figure 3.1: Top view of electromagnet brake system.

provided smoother operation than other materials [9]. Aluminum was the primary material for the shaft and electromagnet housings due to it being easy to machine, inexpensive and non magnetic. The aluminum housings were bolted to an aluminum breadboard which rests on dampers for added vibration isolation. Bushings were chosen over linear steel ball bearing because of the smoothness of the bushings, despite the increased friction. To connect the steel mass to the brass block, an aluminum threaded piece was used. Aluminum was chosen in this case because aluminum is non magnetic and thus it would not interfere with the flux going through the electromagnet to the steel piece. In addition to the aluminum thread, an aluminum alignment piece was placed inside the electromagnet to provide additional alignment. A cross sectional view of the electromagnet is provided in Fig 3.2. To ensure that the steel mass stays in place, a small nut was applied on the opposite end of the steel mass. Finally, a small bias displacement x of 0.02 inches is used to allow for motion of the mass toward the electromagnet. Selection of the bias displacement involves tradeoffs between total allowable travel of the mass and the strength of the force applied by the electromagnet.

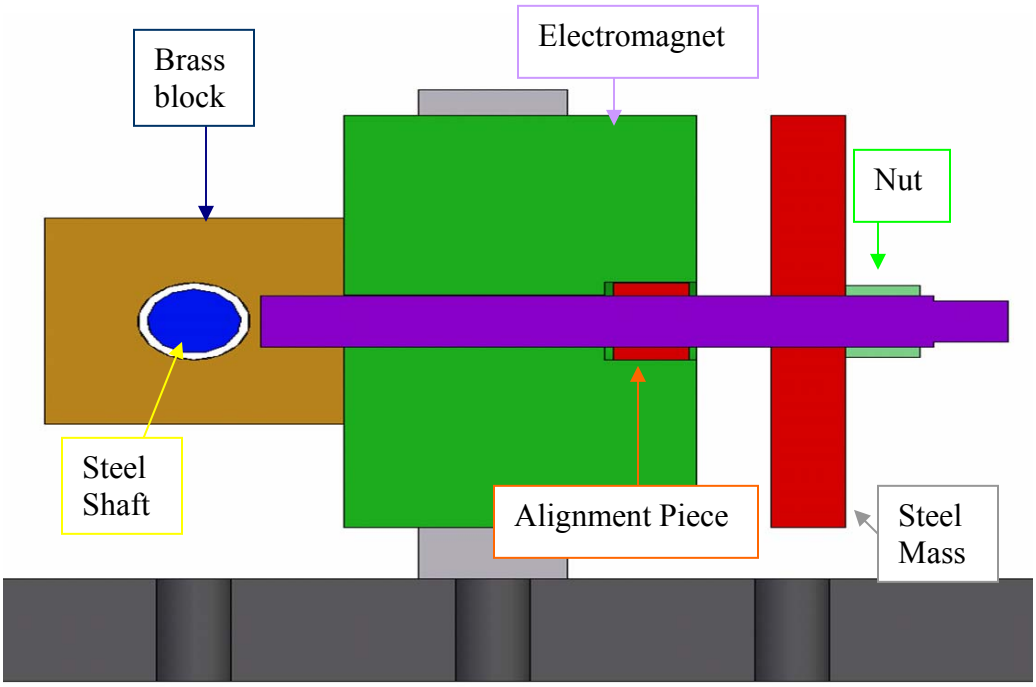

Figure 3.2: Cross-sectional view of the electromagnet brake.

3.2 Equations of Motion

After construction of the design, the system was analyzed so that it could be modeled and controlled. The analysis began with looking at the shaft and all the forces action upon it. The free body diagram of the shaft is provided in Fig 3.3. In this figure several assumptions were made.

Assumptions:

1. Friction at electromagnet contact point is uniform
2. Shaft is constantly in motion
3. The change in friction constants from static to dynamic is small and can be neglected
4. The damping in the system is small enough that it can be neglected
5. The brake is always in contact with the shaft

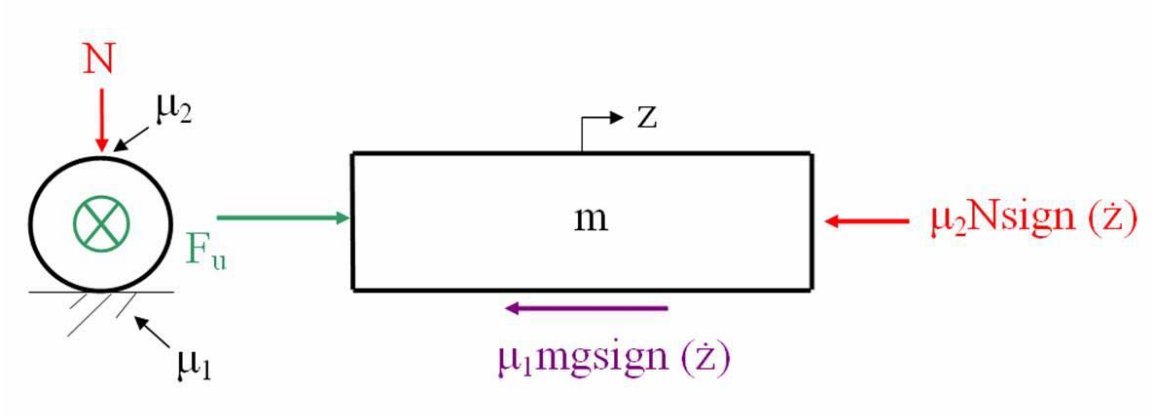

Figure 3.3: Shaft free body diagram.

Applying the five assumptions to Fig 3.3 the following equation of motion becomes

$$m\ddot{z} = F_u - \mu_2 N sign(\dot{z}) - \mu_1 mgsign(\dot{z}) \qquad (3.2.1).$$

The sign of the velocity implies that the direction of the friction forces acting on the shaft depends on the direction of the shaft's movement. To determine the force produced by the electromagnet, the geometry in Fig 3.4 was used. Using this geometry assuming negligible friction and that the brake is always in contact with the shaft the magnetic force takes the form

$$F_{mag} = \frac{(MV)^2 \mu_o A_{gap}}{2(xR)^2} = N \qquad (3.2.2).$$

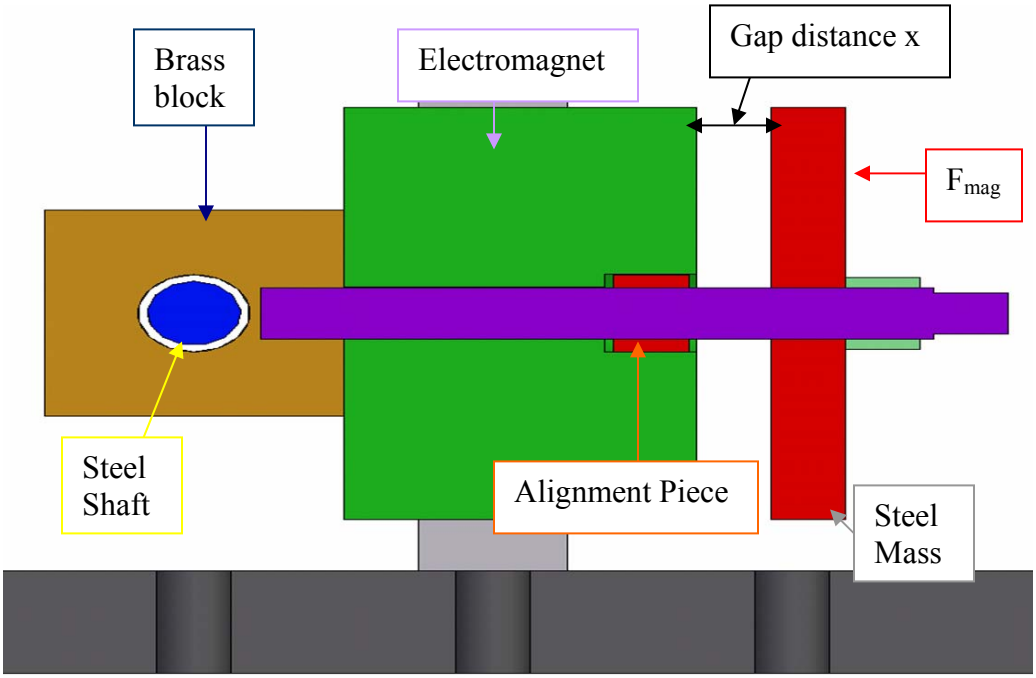

Figure 3.4: Electromagnet geometry.

Combing equations (3.2.1) and (3.2.2), the resultant equation of motion for the shaft takes the form

$$m\ddot{z} = F_u - \mu_2 \frac{(MV)^2 \mu_o A_g}{2(xR)^2} sign(\dot{z}) - \mu_1 mgsign(\dot{z}) \qquad (3.2.3).$$

Chapter 4

Experimental Results

4.1 Experimental Setup

An experiment was setup to characterize the system, as shown in Fig 4.1. Quantities being measured include voltage supplied to the electromagnet, force on the shaft, and displacement of the shaft. A known force was applied to the electromagnet through a pulley, and the voltage of the electromagnet was increased until the change in position was zero. It was assumed that the friction on the pulleys was small enough that it could be neglected.

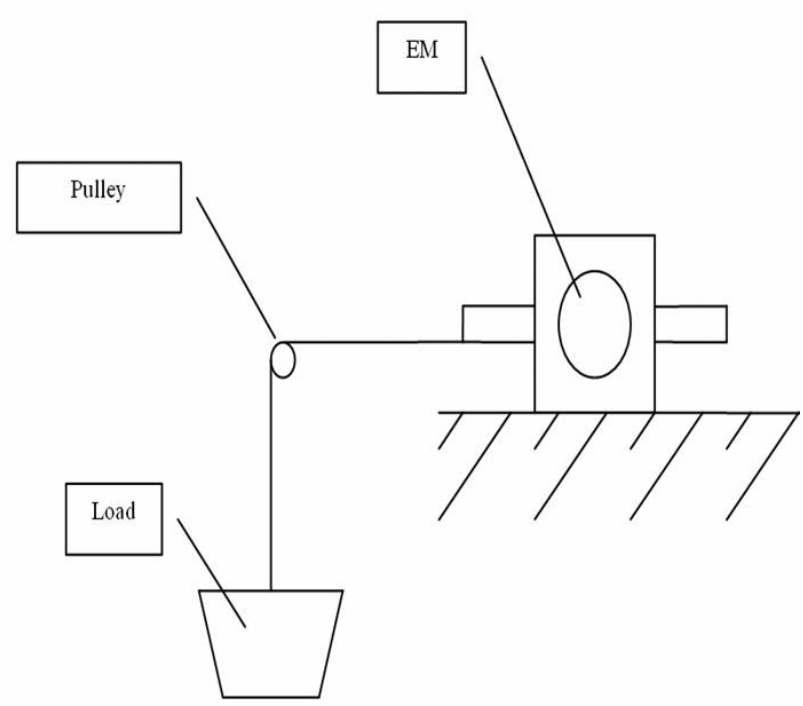

Figure 4.1: Experimental setup used for characterization of electromagnet brake.

4.2 Results

Measurements were conducted for a range of forces between 2.2 – 16.2 N at 1 N increments. The data from these ten tests are shown in Fig 4.2. It is noted near a voltage of 1.8 V, small changes in voltage result in large changes in force. This implies that a small change in displacement must have occurred. To illustrate, Figs 4.3 and 4.4 were created by using the force equation of the electromagnet (2.1.3) and then multiplying by a scaling factor to match the maximum output recorded from the data as a function of voltage. In Fig 4.3, the output force of the electromagnet that opposes displacement of the shaft was plotted as a function of the gap in the electromagnet. As expected, the output force increases with increasing voltage. The figure suggests that any specific force can be achieved at different positions with different corresponding voltages. Fig 4.4 also illustrates this issue, but where each curve represents a different displacement value. As the displacement increases the output force also increases.

It is emphasized that a ten percent change in position corresponds to the magnetic piece moving 0.097 mm. However, inspection of Fig 4.4 does not immediately reveal how drastic the change in forces can be for a small change in displacement. A closer view of the forces versus voltage is shown in Fig 4.5 where only two possible paths indicated in blue and red have been displayed of the many possibilities. In this case the magnetic piece does not change its position until after 3.1 V. Nonetheless when it does change by 0.097 mm, there is a significant increase in force of approximately 4 N. The second case has an initial change in displacement. The change in force is not as drastic as in the first case but there is a significant difference. These significant differences in forces make it difficult to predict what the output force will be as a function of voltage. Furthermore, the measurements are not an accurate representation of system behavior because in the tests the brake transitions between forces governed by static and dynamic coefficients of friction.

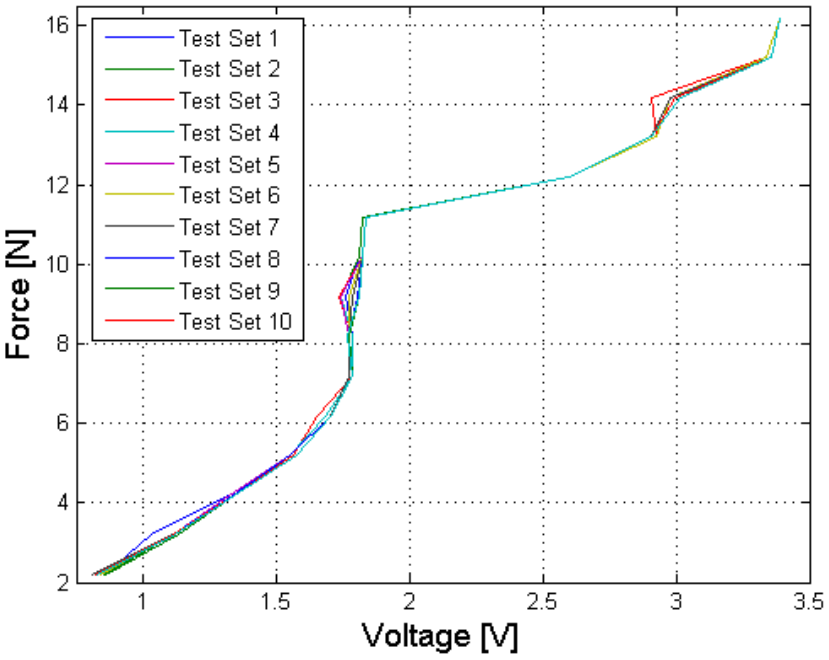

Figure 4.2: Experimental measurements conducted on the electromagnetic brake.

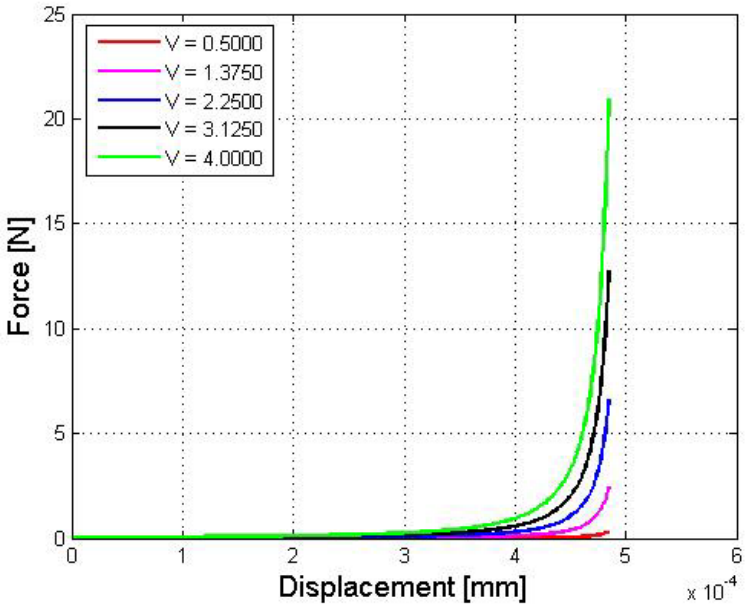

Figure 4.3: Theoretical electromagnet force versus displacement.

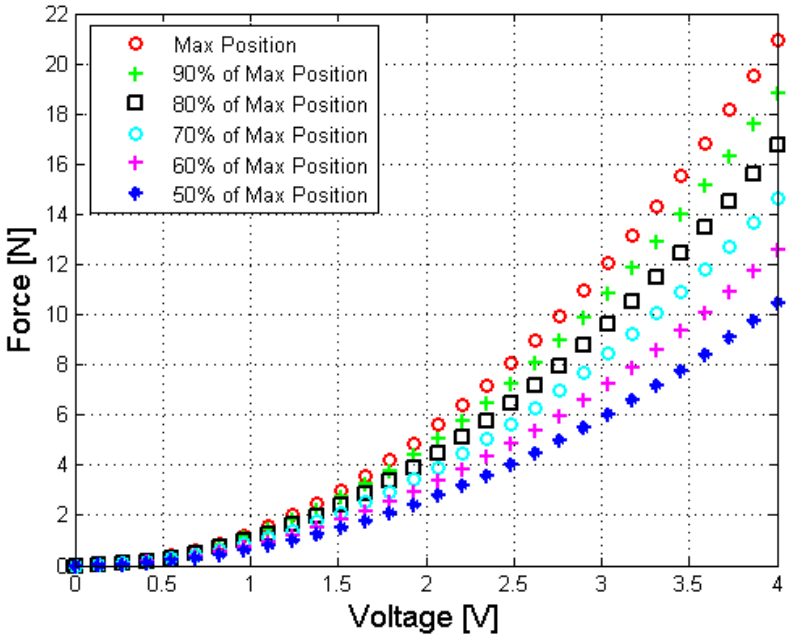

Figure 4.4: Theoretical electromagnet force versus voltage.

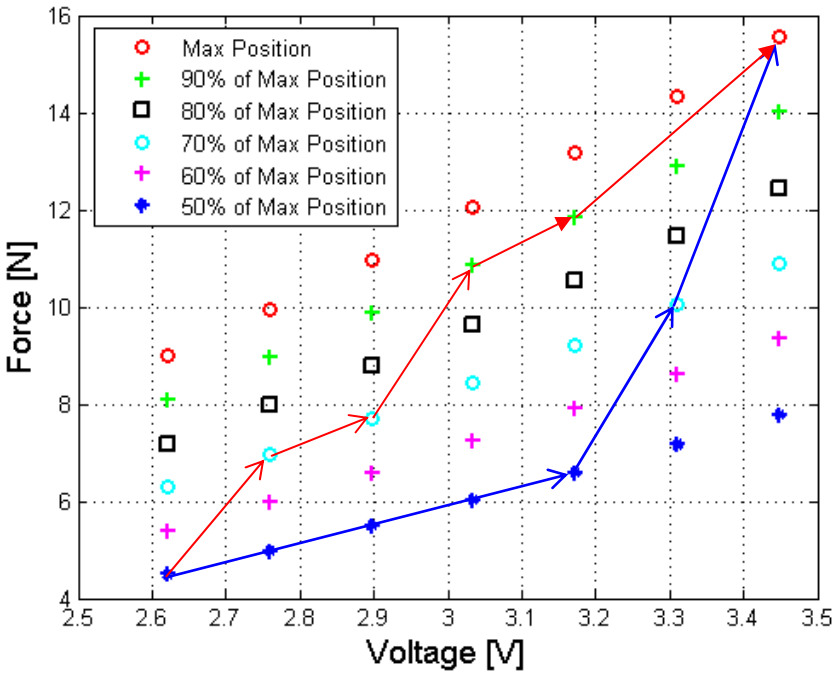

Figure 4.5: Electromagnet path illustration indicated by the red and blue lines.

The electromagnet that was used for this experiment had a rated holding force of 467 N while the maximum recorded load was only 25.6 N. There are two mains reasons to account for theses differences. First, the electromagnet never achieves maximum displacement. The gap between the brass block and the steel shaft is smaller than the gap between the steel mass and the electromagnet. Thus the electromagnet can never completely close although it can get close. The second reason for the discrepancy is due to some additional misalignment. An illustration has been provided in Fig 4.6. Despite adding the alignment piece inside the electromagnet, there is still some misalignment. The result was one surface of the steel piece was closer to the electromagnet and thus increasing the flux in this small region. To further prevent misalignment one solution would be to support the brass block and steel mass. The misalignment can be fixed by providing low friction support beneath the brass block and moving iron as shown in Fig 4.7 or by moving iron's shaft to slide within a bushing.

Finally, to ensure accurate prediction of the force from the electromagnet it will be necessary to measure the displacement of the mass and minimize the change in displacement. Measurement of the displacement could be achieved by using a laser measurement sensor or an LVDT. Knowing the input voltage, displacement and the constants associated with the electromagnet should result in improvement of the experimental data's ability to follow the theoretical values more closely. Minimization of the displacement could be realized by having a spring opposing the displacement of the electromagnet. The spring would have to be calibrated such that it would not be stronger than the electromagnet and behave linearly.

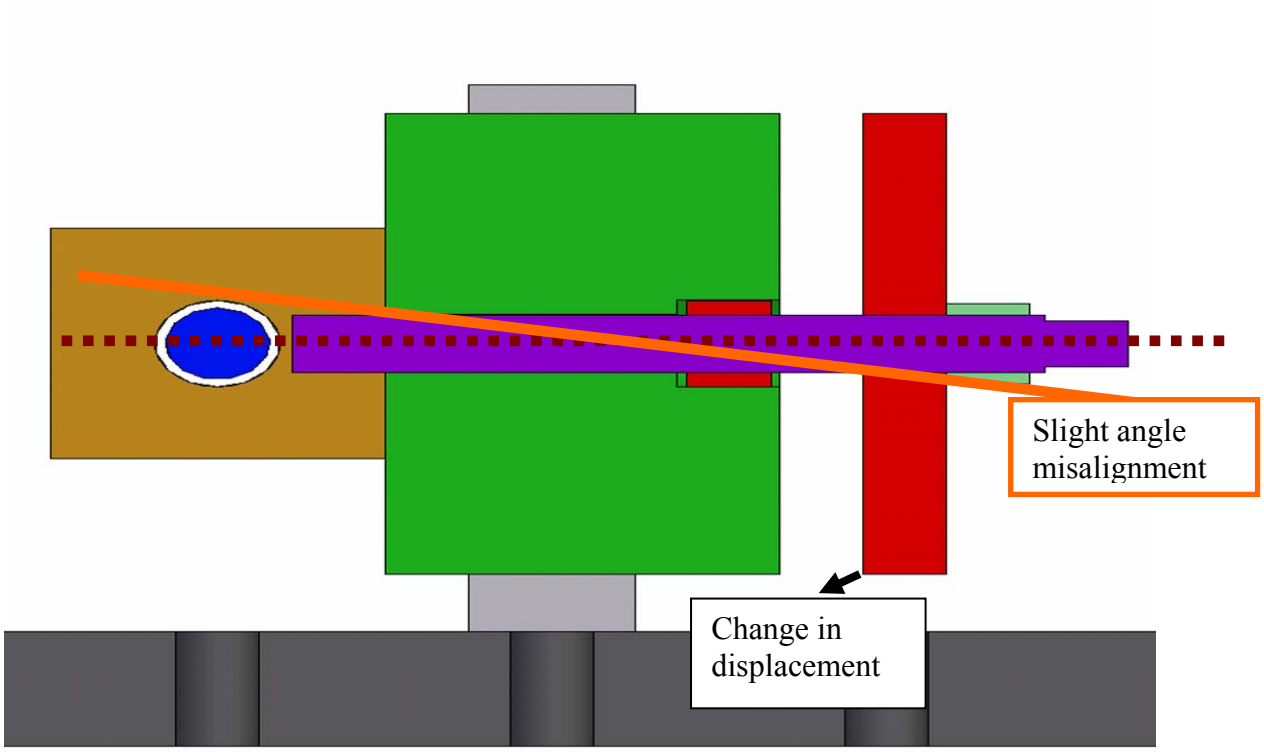

Figure 4.6: Electromagnet misalignment.

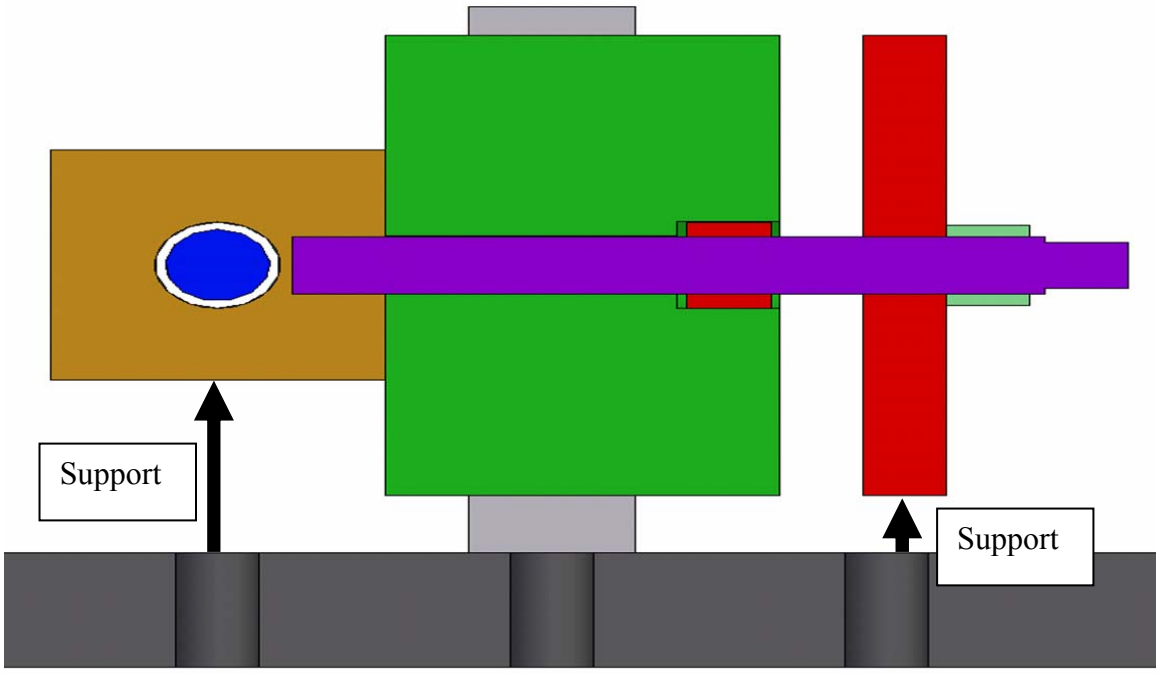

Figure 4.7: Proposed solution to fix the electromagnet misalignment.

To address the discrepancy between experimental data and theory, and improve the repeatability of the measurements, a new experimental testing methodology is needed. In the new experimental setup, which is shown in Fig 4.8, a known voltage is applied to the magnet and a horizontal MTS machine is used to apply a force onto the shaft.

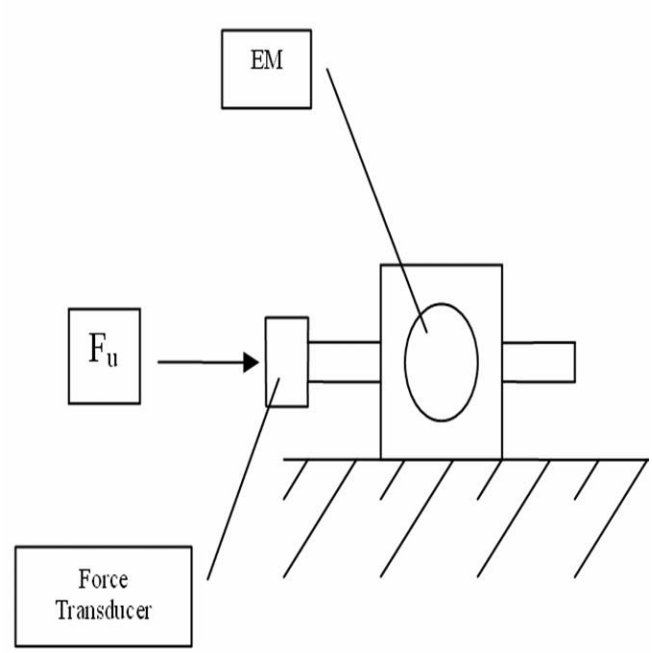

Figure 4.8: Proposed experimental setup.

Chapter 5

Control

5.1 Control Methodology

Although an accurate model for the system was not realized due to errors in testing, it was still necessary to design a controller that could track a desired signal. Therefore to model the system a theoretical curve was used based on having a small change in position of the magnet piece. The curve that was used to implement the controller is shown in Fig 5.1. To model the epidural as a function of displacement, the force versus displacement curve shown in Fig 5.2 was taken from the literature [3]. After obtaining the desired signal, a Simulink model was created using the equation of motion found in equation (3.2.3). The Simulink diagram can be found in the Appendix. It should be noted that the Simulink model does not account for the dynamics of the electrical circuit since it was assumed that the dynamics of the circuit were sufficiently fast that they could be neglected but it would be useful to have the dynamics of the electrical circuit in the final model. The transfer function relation input voltage to output has the form

$$\frac{V}{I}(s) = \frac{1/L}{s + R/L} \qquad (5.1.1).$$

A PI controller was used to track the desired signal. A PI controller was chosen because it aids in significantly reducing the error of the signal and can be easy implemented using dSPACE [10]. The non-linear nature of the electromagnet required using an iterative approach to determining the gains of the systems rather than an analytic approach. Initially, the integral control was set to zero and the proportional control was set to the maximum value that would not saturate the actuator. The proportional control gain was then slightly reduced and integral control was added until desirable results where obtained. These control values where applied to three different input signals from the

user. Each input signal corresponded to a different type of person operating the device. Detailed explanations of the results are provided in the following sections.

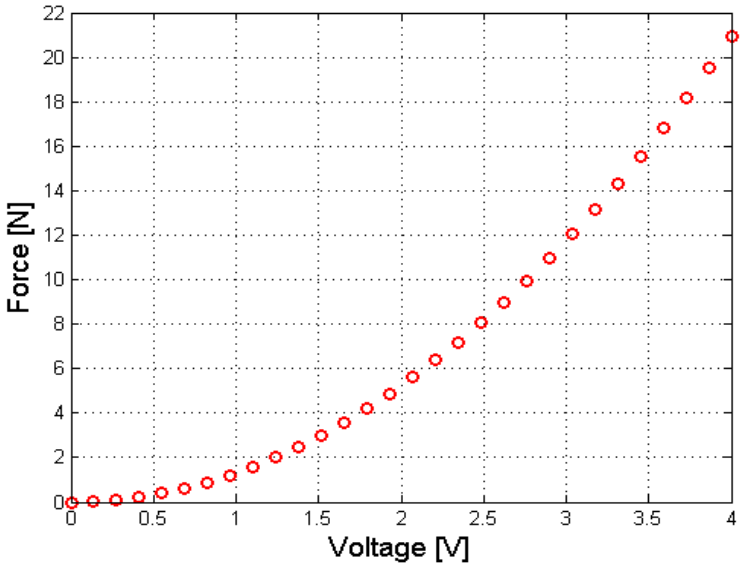

Figure 5.1: Theoretical electromagnet force versus voltage.

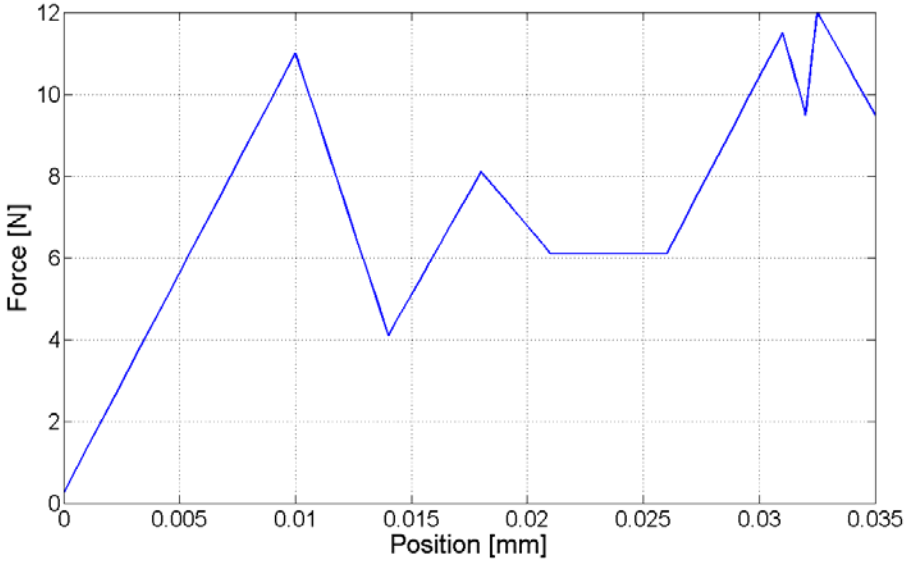

Figure 5.2: Desired epidural simulation.

5.1.1 Forceful Entry

To simulate the extreme case of forceful entry of the needle, a large ramp input signal was sent into the device as shown in Fig 5.3(a). While this is an unlikely scenario in practice, a ramp input helps to characterize the dynamics of the system. The resultant tracking force versus time is shown in Fig 5.3(b), while the percent error of the device as a function of time is shown in Fig 5.3(c). Finally, the percent error versus time after 0.2 seconds is shown in Fig 5.3(d). It is noted that after 0.2 seconds the percent error is always less than six percent. The only other time when the percent error increases above one percent is after 0.2 seconds when there are sharp changes in the track signal. However, theses changes in error are small enough to be acceptable.

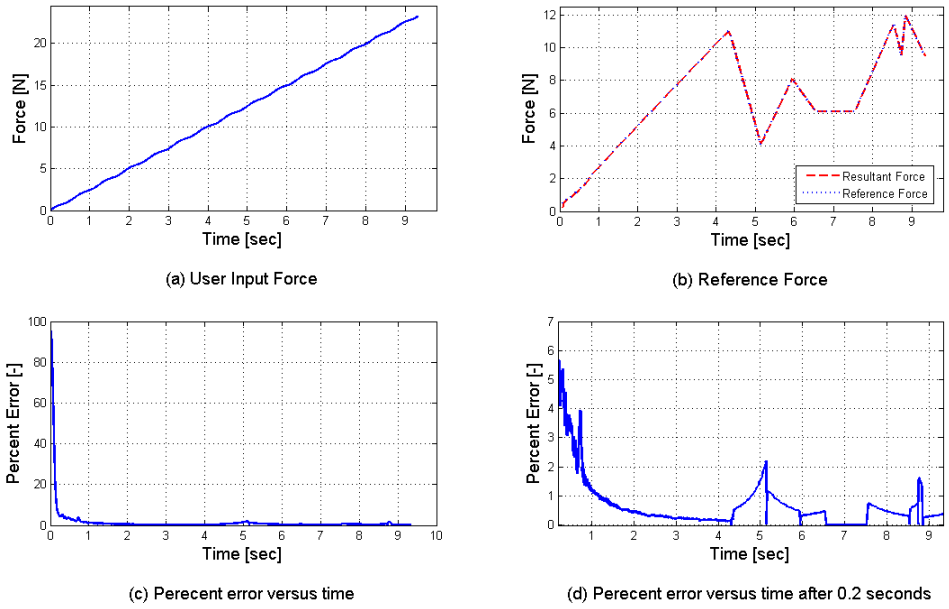

Figure 5.3: Forceful entry of needle.

5.1.2 Unsteady Hand

To simulate the case of a user with an unsteady or shaky hand but constantly moving forward, a ramp input was used in addition to a high frequency low amplitude sine wave that was added to it. The user input signal, reference force, and percent error are shown in Fig 5.4. Although, the percent error is high initially it is always less than seven percent after 0.2 seconds. The only other time when the percent error increases above one percent after 0.2 seconds is when there are sharp changes in the track signal. However, theses changes in error are small enough to be acceptable.

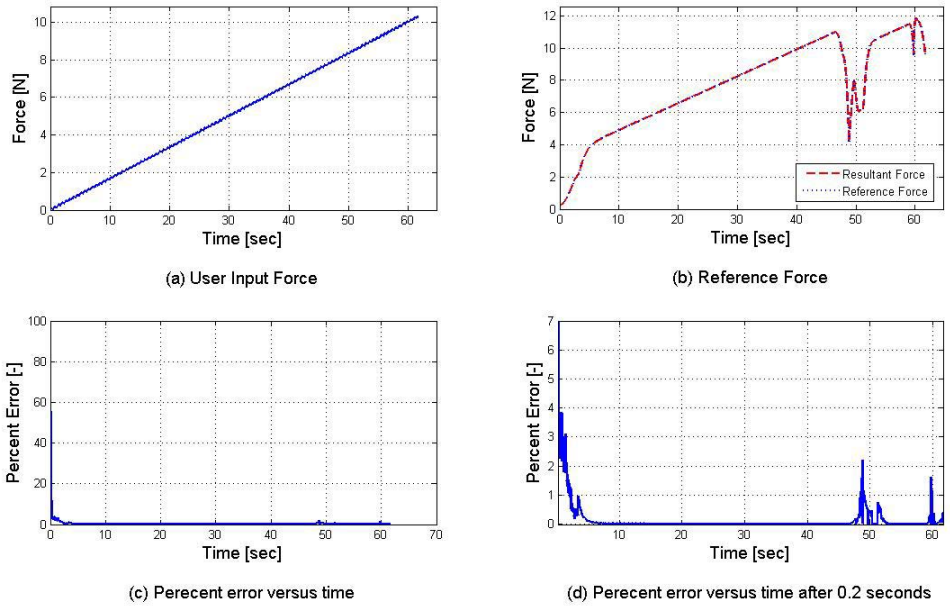

Figure 5.4: Unsteady hand.

5.1.3 Stop and Go

Finally, to simulate a user operating the device in small bursts but constantly moving forward, a repeating, increasing ramp signal was used in addition to a low frequency small amplitude sine wave. As in the other cases, the user input signal, reference force, and percent error were plotted together in the same graph and are shown in Fig 5.5. The percent error is initially high but after 0.2 seconds the percent error is small and in this case it is the smallest of the three responses, always less than five percent. This simulation took more time but the results were improved.

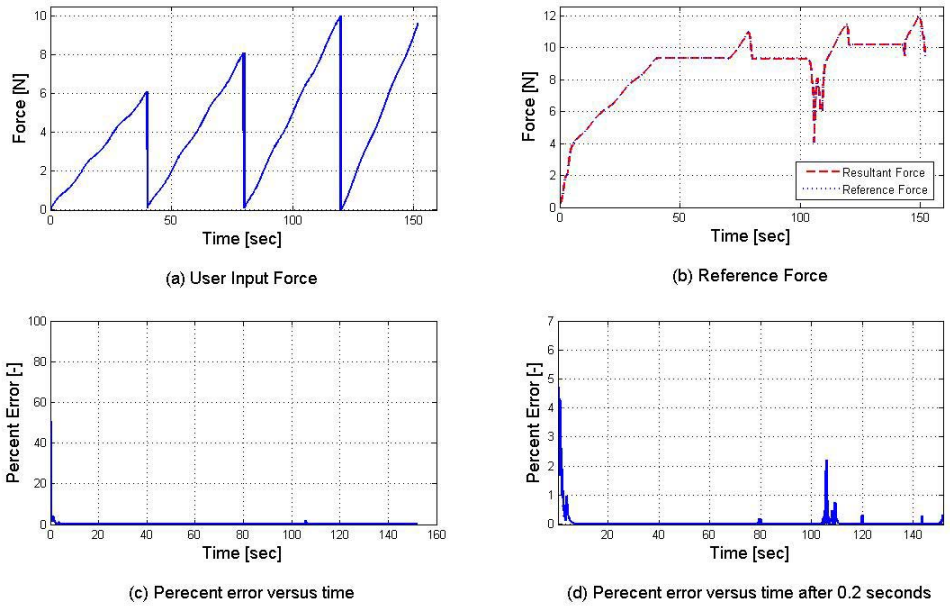

Figure 5.5: Stop and go input.

Chapter 6

Conclusions and Future Work

This document presents a new and exciting device for enhancing the fidelity of epidural needle insertion virtual reality simulations. Experimental measurements conducted at the Smart Materials and Structures Lab demonstrate the feasibility of the device, especially in regard to its ability to simulate contact between the needle and bone, which largely represents the limiting condition for existing cable-operated devices. Notwithstanding, a number of aspects need to be improved before the device can be implemented in a commercial system. To that end, a new methodology is proposed along with design changes aimed at improving the repeatability of the system's response and addressing misalignment issues in the electromagnet. Initial steps were taken toward developing a device controller. While the simulations are promising, the abovementioned issues significantly compromise the accuracy of the results. The steps described above will surely enhance the ability of the controller to establish the drive voltage required for the device to track a given force profile.

Bibliography

[1] L.B. Rosenberg and D. Stredney, "A Haptic Interface for Virtual Simulation of Endoscopic Surgery," *Health Care in the Information Age,* pp. 371-387, 1996.

[2] L. Hiemenz, D. Stredney and P. Schmalbrock, "Development of The Force-Feedback Model for an Epidural Needle Insertion Simulator," *Medicine Meets Virtual Reality,* pp.272-275, 1998.

[3] B.G. Covino, and D.B. Scott, *Handbook of Epidural Anesthesia and Analgesia*, Grune & Strattion Inc, Orlando, 1985.

[4] J. Magil, B. Anderson, G. Anderson, P. Hess, and S. Pratt, "Multi-Axis Mechanical Simulator for Epidural Needle Insertion," *International Symposium on Medical Simulation*, 2004

[5] J.E. Usubiaga, *Neurological Complications Following Epidural Anesthesia*, Little, Brown and Company, Boston, 1975.

[6] D. Blezek, R. Robb, and D. Martin, "Virtual Reality Simulation of Regional Anesthesia for Training of Residents," *Proc. of 33rd Hawaii International Conference on System Sciences,* 2000.

[7] D. Halliday, R. Resnick, and J. Walker, *Fundamentals of Physics Extended*, John Wiley & Sons Inc, New York, 1997.

[8] G. Rizzoni, *Principals and Applications of Electrical Engineering*, McGraw-Hill, New York, 2000.

[9] I.V. Kragelski, V.V. Alisin, N.K. Myshkin, and M.I. Petrokovets, *Tribology – lubrication, friction, and wear*, Mir Publishers, Moscow, 2001.

[10] G. F. Franklin, J.D. Powell, and A. Emami-Naeini, *Feedback Control of Dynamic Systems*, Prentice Hall, New Jersey, 2002.

Appendix

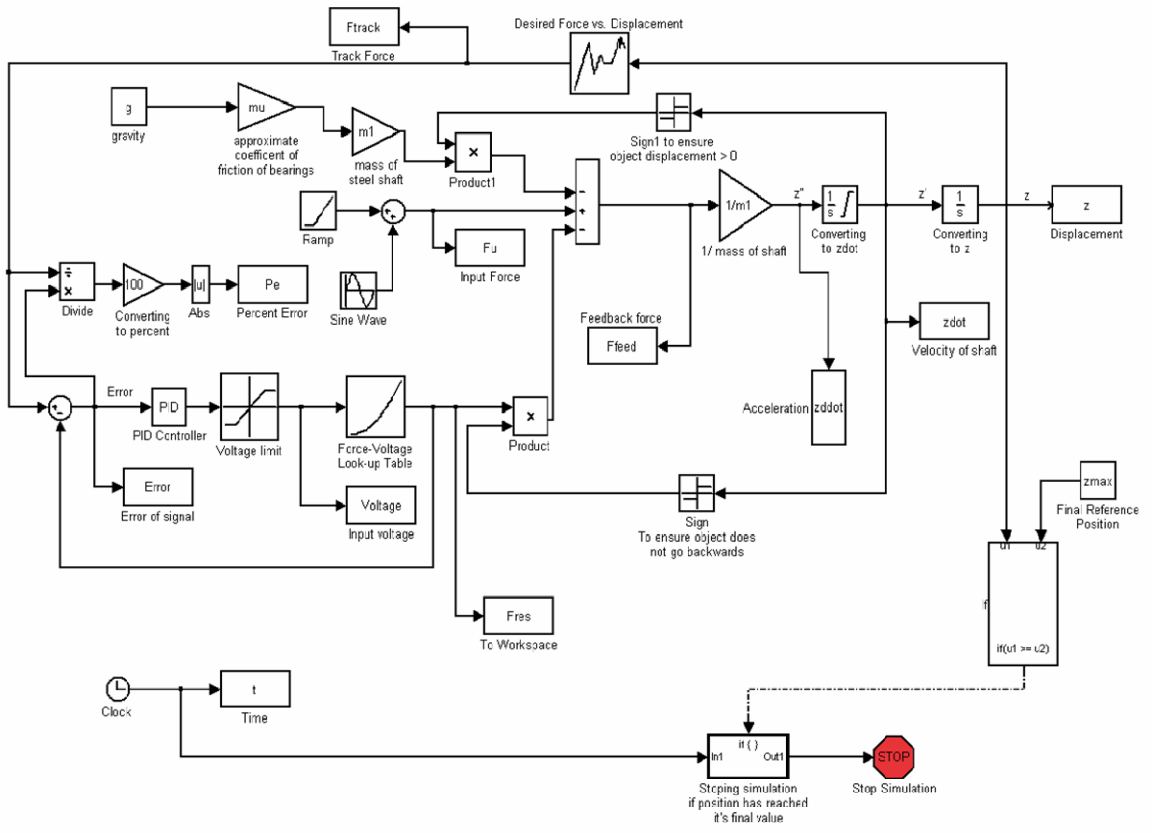

Figure 8.1: Epidural simulink model.